Journal of Ceramic Processing Research. Vol. 22, No. 4, pp. 436~440 (2021)
(Received 25 November 2020, Received in revised form 13 February 2021, Accepted 2 March 2021)
https://doi.org/10.36410/jcpr.2021.22.4.436

J O U R N A L O F
Ceramic Processing Research

Tunable green-yellow-red light properties of $NaY(WO_4)_2$: Mn^{2+}, Dy^{3+}, Eu^{3+} phosphors excited with 365 nm LED

Yonghua Wu[a,*], Fugui Yang[b], Hao Zhang[b], Fengpo Yan[b] and Ruijuan Zuo[c]
[a]*College of Electronic and Information science, Fujian Jiangxia University, Fuzhou, Fujian, 350108, P.R. China*
[b]*Matimatical Institution, Fujian Jiangxia University, Fuzhou, Fujian, 350108, P.R. China*
[c]*College of Mathematics and Informatics, Fujian Normal University, Fuzhou, Fujian, 350117, P.R. China*

By the solid-state reaction method, the $NaY(WO_4)_2$: Mn^{2+}, Dy^{3+}, Eu^{3+} phosphors are synthesized successfully. The sample's phase-structure and morphology have been characterized by XRD and EDS. The concentrations of Mn^{2+}, Dy^{3+}, Eu^{3+}, Y^{3+} and W^{6+} are measured by ICP, The result implies that the doped process of Mn^{2+}, Dy^{3+} and Eu^{3+} is very easy in host $NaY(WO_4)_2$. The absorption and excited spectra are presented, The absorption spectrum of Mn^{2+} is always broad, but the Dy^{3+}, Eu^{3+}has relatively sharp absorption peaks.Using the commercial LED of 365 nm wavelength as the excitation light, the emission spectra with different doped concentrations ratios of Mn^{2+} are obtained. The Mn^{2+} doping reduces the emission intensity of Dy^{3+},also it has meaningful influence on the tunable green-yellow-red LED.The high doped concentration of Mn^{2+} can guarantee the emission intensity of 546 nm enough.

Keywords: Solid-state reaction, XRD, Phase-structure, LED, Absorption spectrum, Emission intensity

Introduction

Recently, the LED technology has been applied in many fields such as lighting, display, health, agriculture, transportation, environment, etc. In the phosphor family, the rare-earth phosphors have large number of energy levels and excited wavelengths suitable for the ultra-visible light, and occupy the vast majority such as NaY $(WO_4)_2$:Yb/P [1], $NaLa(WO_4)_2$:Eu^{3+} [2], $ZnWO_4$:Sm/Eu/Tb/Dy [3], $NaLa(WO_4)_2$:Dy^{3+} [4, 5], $ZnWO_4$: Cr^{3+}/Mn^{2+}/Cu^{2+} [6]. the Eu^{3+} ion is important activators due to its red emission band corresponding to the transition of $^5D_0 \rightarrow {}^7F_{0\text{-}4}$ [7]. the Dy^{3+} has been widely used to generate the blue, yellow and red light, corresponding to the transition of $^4F_{9/2} \rightarrow {}^6H_{13/2}$ [8], because of its plentiful absorption and emission spectra.. Mn^{2+} has been widely used to generate the green light [9, 10]. By doping different ions, a variety of fluorescent materials with rich colors and satisfying different uses can be obtained [11].

Considering of the character of Mn^{2+} [12], Dy^{3+} [13], Eu^{3+} [14], in the work, we attempt to investigate the fluorescence performance of $NaY(WO_4)_2$: Mn^{2+}, Dy^{3+}, Eu^{3+} phosphors and discuss the mechanism of tunable green-yellow-red emission. We chose the $NaY(WO_4)_2$ as the host because that the tungstate has many merits such as good thermal stability, environmental safety, simple synthesis process and low synthesis temperature (~1,000 °C) [15-19]. Compared with fluoride and sulfide, the oxide is environmentally friendly and easy to prepare. Particularly, the tungstate root $[WO_4]^{2-}$ has good blue absorption and emission bands, which contributes to the cross-energy levels transition[20-21]. Mn^{2+} ions not only have a rich and broad absorption band, they are often used as doping ions to improve fluorescence performance.

Using the host of $NaY(WO_4)_2$, the Dy^{3+} (0.091 nm) and Eu^{3+}(0.096 nm) can easily replace the Y^{3+} (0.09 nm)due to the similar electronic structure (4f), and the Mn^{2+} (0.067 nm) can also occupy the site of Na^{1+} (0.102 nm). More important, some of the absorption peaks of Mn^{2+}, Dy^{3+}, Eu^{3+} are overlapped such as 365 nm, which make the excitation source is single and simple, so we use 365 nm as the excitation source.

The luminescence of $NaY(WO_4)_2$:Dy^{3+}, Eu^{3+}, Zn_2SiO_4: Mn^{2+}, Eu^{3+}, Dy^{3+}, $NaY(WO_4)_2$:Eu^{3+} have been investigated in earlier paper [22-24]. But till now, the phosphor of $NaY(WO_4)_2$:Mn^{2+}, Dy^{3+}, Eu^{3+} has not been investigate yet. And so, in the work, we introduce the Mn^{2+} in $NaY(WO_4)_2$:Dy^{3+}, Eu^{3+} .The adjustment mechanism of Mn^{2+} ions in $NaY(WO_4)_2$:Mn^{2+}, Dy^{3+}, Eu^{3+} phosphors has been also discussed. The result shows that the $NaY(WO_4)_2$:Mn^{2+}, Dy^{3+}, Eu^{3+} phosphors have good tunable green-yellow-red light with better performance.

Experimental Section

Power samples of $NaY(WO_4)_2$:xMn^{2+}, yDy^{3+}, zEu^{3+} (x = 1, 2, 6, 8, 15 at%; y = 4 at%; z = 4 at%) phosphors

*Corresponding author:
Tel : +86-189-0591-1552
Fax: +86-591-22823853
E-mail: wuyonghua@fjjxu.edu.cn

were fabricated via a solid state reaction method. The starting materials are $MnCO_3$ (99.99%, 0.5-1 μm), Na_2CO_3 (99.995%, 0.2-0.5 μm), Eu_2O_3 (99.99%, 0.5-1 μm), Y_2O_3 (99.99%, 0.5-1 μm), Dy_2O_3 (99.99%, 0.5-1 μm), WO_3 (99.98%, 0.1-0.5 μm). The reaction equation is as follows:

$$0.5xMnCO_3 + (1\text{-}0.5x)Na_2CO_3 + 2WO_3 + 0.5yDy_2O_3 + 0.5zEu_2O_3 + 0.5(1\text{-}y\text{-}z)Y_2O_3 \rightarrow xMn^{2+}, yDy^{3+}, zEu^{3+}: NaY(WO_4)_2 + CO_2 \uparrow \quad (1)$$

Each mixture of starting materials were mixed homogeneous by an agate mortar and then loaded into an Al_2O_3 crucible. After that the mixture was sintered in a tube furnace at 1,000 ± (5) ºC for 4 h in a CO-reducing atmosphere. As the reaction finished, the vessel was naturally cooled down to room temperature, and the white precipitation was washed with distilled water. After that, the precipitate was dried at 70 ºC for 7 h. Finally the $NaY(WO_4)_2$: Mn^{2+}, Dy^{3+}, Eu^{3+} micro-structures were obtained through a calcination process at 600 ºC for 1 h.

The purity and phase structure of the sample was identified by XRD using Rigaku Miniflex 600 diffractometer with graphite-monochromatized Cu-Ka radiation (λ = 0.1540 nm). The 2θ angle ranged from 15º to 75º, and the scanning step size was 0.02º. The concentrations of Mn^{2+}, Dy^{3+}, Eu^{3+}, Y^{3+}, W^{6+} ions were measured by inductively coupled plasma atomic emission spectrometry method (ICP-AES instrument, Agilent ICPOES730). The micro-structure was measured by EDS (Energy Dispersive Spectrometer). The absorption spectra were recorded by Shimadzu UV-2600 UV-VIS-NIR spectrophotometer. The excitation was measured by Edinburgh Instruments FLS980 fluorescence spectrometer. Excited with 365 nm LED, the emission spectra with different concentrations of Mn^{2+}, Dy^{3+}, Eu^{3+} were measured by USB2000+ spectrometer (Ocean Optics Ltd.).

Results and Discussion

Structure and morphology characterization

The powder XRD patterns of concentration NaY $(WO_4)_2$:xMn^{2+}, yDy^{3+}, zEu^{3+} (x = 4 at%; y = 4 at%; z = 4 at%) phosphor were measured to identify the crystal structure of products and are shown in Fig. 1. The XRD diffractive peak positions of studied sample match well with JCPDS #48-0886 for body-centered host $NaY(WO_4)_2$ of tetragonal phase with the space group I41/a and its lattice parameter values are a = 0.5205 nm, b = 0.5205 nm, c = 1.1251 nm, α = β = γ = 90º, thus indicating the achievement of the target products.

From the Fig. 1, we can conclude that doping trivalent ions (Mn^{2+}, Dy^{3+}, Eu^{3+}) into the host $NaY(WO_4)_2$ will keep single phase and the doping process and the dopant

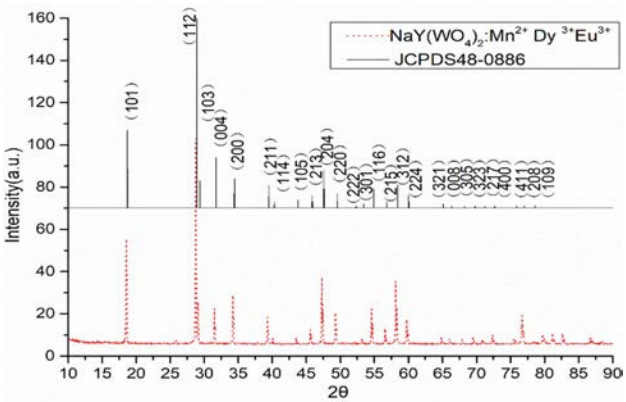

Fig. 1. XRD pattern for the phosphor $NaY(WO_4)_2$: xMn^{2+}, yDy^{3+}, zEu^{3+} (x = 4 at%; y = 4 at%; z = 4 at%), and the standard diffraction pattern in JCPDS card No.48-0886.

concentration is the studied concentration region do not affect the structural properties of pure $NaY(WO_4)_2$.

The morphology of the $NaY(WO_4)_2$:xMn^{2+}, yDy^{3+}, zEu^{3+} (x = 4 at%; y = 4 at%; z = 4 at%) phosphors calcined at 800 ºC is showed in Fig. 2(a). The measurement in the Fig. 2(a) is 5 um. It can be seen from the Fig. 2(a) that the sample is powdery and uniformly distributed. The size is 1-2 um. SEM showed that we successfully prepared our samples. Through the change of CPS, it can be seen that the sample is evenly distributed in the longer size range of 15 um. The line-EDS spectra were dealt with the maximum 15 KV voltage and 16 μm length. scanning distance vs counts per-second is showed in Fig. 2(b). SEM images exhibit distorted spherical and rectangular sharp. Almost unchanged morphology are observed. This fact illustrates that the doped ions at the present level does not destroy the initial micro-crystal structure, and the stable $NaY(WO_4)_2$ microstructures can be reproducibly obtain. the sample keeps still pure single crystal phase.

The concentrations of Mn^{2+}, Dy^{3+}, Eu^{3}, Y^{3+}, W^{6+} ions were tested by ICP ($NaY(WO_4)_2$:4at%Mn^{2+}, 4at%Dy^{3+}, 4at%Eu^{3+}). The constant volume is 25 mL. The used mass is 0.0509 g. It added the 10 mL aqua regia in the samples, in order to make the synthesis more uniform and then samples are heated to 180 ºC for chemical reaction. The sample was cooled down for testing after complete reaction. The measured amount of Mn^{2+}, Dy^{3+}, Eu^{3+}, Y^{3+}, W^{6+} were shown as the following:

Mn^{2+}: 2708.5 mg/kg, Dy^{3+}: 7801.6 mg/kg, Eu^{3+}: 7704.6 mg/kg, Y^{3+}: 85741.6 mg/kg, W^{6+}: 833295.7 mg/kg

So the concentrations of Mn^{2+}, Dy^{3+}, Eu^{3+}, Y^{3+}, W^{6+} are obtained to be 0.0493 mol/Kg, 0.048 mol/kg, 0.0507 mol/kg, 0.9638 mol/kg, 4.5327 mol/kg. The measured concentration mole ratio of Mn^{2+}, Dy^{3+} and Eu^{3+} is identical with the initial synthesis concentration ratios (1:1:1). The result implies that the doped process of Mn^{2+}, Dy^{3+} and Eu^{3+} is very easy in host $NaY(WO_4)_2$.

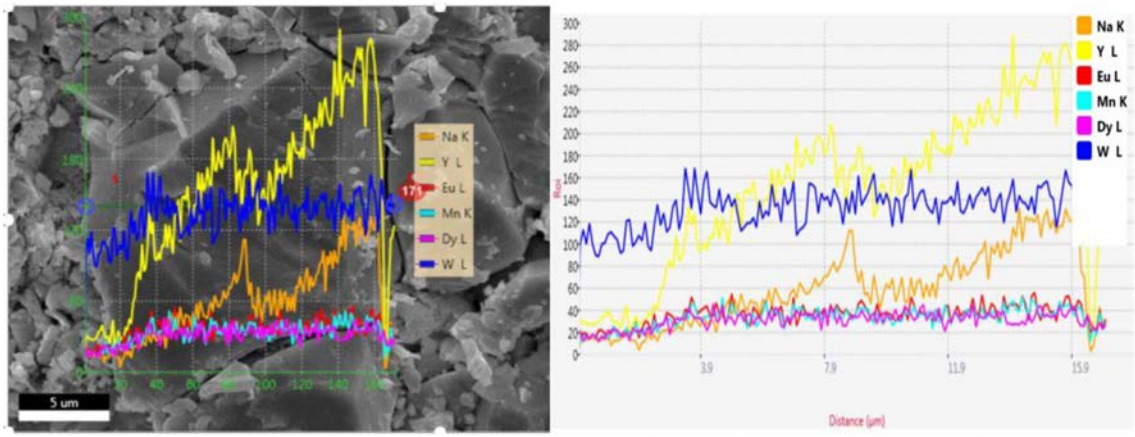

(a) SEM image (b) distance vs the counts per-second (cps)

Fig. 2. SEM image for $NaY(WO_4)_2$ microstructure coped with 4 at% Mn^{2+}, 4 at% Dy^{3+}, 4 at% Eu^{3+}.

Spectra properties of $NaY(WO_4)_2$:Mn^{2+}, Dy^{3+}, Eu^{3+} phosphors

The absorption spectra of the $NaY(WO_4)_2$: xMn^{2+}, yDy^{3+}, zEu^{3+} (x = 6 at%; y = 4 at%; z = 4 at%) phosphors are measured in Fig. 3. Many absorption peaks are obtained from 270-500 nm, these peaks are concentrated at 332 nm (Dy^{3+}), 345 nm (Dy^{3+}, Mn^{2+}), 347 nm (Mn^{2+}), 365 nm (Eu^{3+}), 367 nm(Mn^{2+}), 395 nm (Eu^{3+}), 465 nm (Dy^{3+}, Mn^{2+}). Many peaks of Dy^{3+}, Eu^{3+} and Mn^{2+} are overlapped. The absorption spectrum of Mn^{2+} is always broad, but the Dy^{3+}, Eu^{3+}has relatively sharp absorption peaks.

The excitation spectrum of sample ($NaY(WO_4)_2$: xMn^{2+}, yDy^{3+}, zEu^{3+} (x = 6 at%; y = 4 at%; z = 4 at%)) with 575 nm emission has been measured and are shown in the upper of Fig. 3, seven peaks of Dy^{3+} concentrated at 325 nm, 352 nm, 366 nm, 395 nm, 430 nm, 450 nm and 476 nm were observed. When the Mn^{2+} doped in the phosphors, the absorption peaks change heavily. Two strong excitation intensities are found in 365 nm and 395 nm. Compared with the absorption spectrum, the 365 nm is more suitable than 395 nm because of Mn^{2+}. Also 365 nm has more stronger intensity, it is corresponding to the transition of $^7F_0 \rightarrow {}^5D_4$ (Eu^{3+}), $^6A_1 \rightarrow {}^4T_2$($Mn^{2+}$), $^6H_{15/2} \rightarrow {}^4M_{19/2}$($Dy^{3+}$).

The excitation source is used with the 365 nm LED, the emission spectra are shown in Fig. 4. Three emission peaks center at 546 nm ($^4T_2 \rightarrow {}^6A_1$ (Mn^{2+})), 575 nm ($^4F_{9/2} \rightarrow {}^6H_{13/2}$ (Dy^{3+})), 613 nm-617 nm ($^5D_0 \rightarrow {}^7F_0$ (Eu^{3+})) are observed. In order to facilitate comparison, the 617nm emission light peak intensity is used as a fixed value for comparison. With the increasing doped concentration of Mn^{2+}, the emission intensity of 546 nm ($^4T_2 \rightarrow {}^6A_1$ (Mn^{2+})) becomes stronger. With the decreasing doped concentration of Mn^{2+}, the emission intensity of 575 nm ($^4F_{9/2} \rightarrow {}^6H_{13/2}$ (Dy^{3+})) becomes stronger. The Mn^{2+} doping reduces the emission intensity of Dy^{3+}, mainly the reason is that the energy absorbed by Dy^{3+} is transferred to Mn^{2+}. The main energy transfer way is resonance transmission. And so, we can obtain the tunable

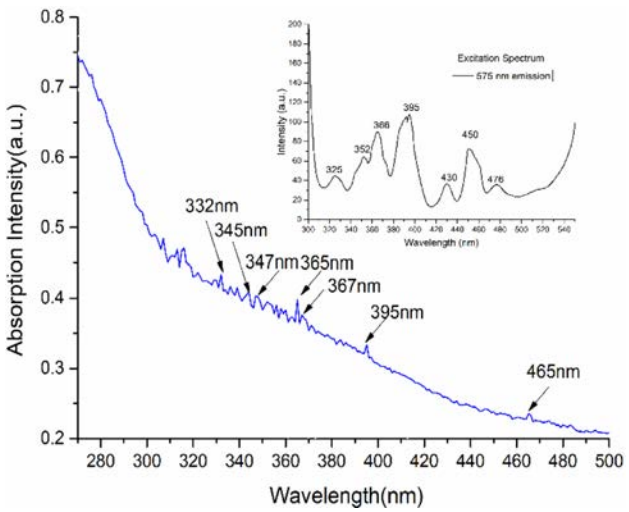

Fig.3. The absorption spectra of $NaY(WO_4)_2$: xMn^{2+}, yDy^{3+}, zEu^{3+} (x = 6 at%; y = 4 at%; z = 4 at%) phosphors; excitation spectrum with 575 nm emission is at the upper.

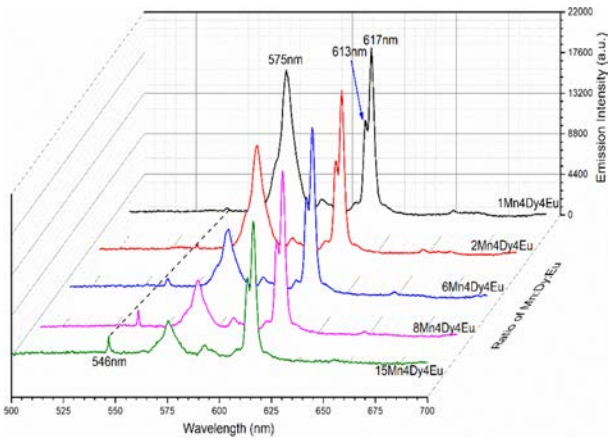

Fig. 4. Emission spectra of $NaY(WO_4)_2$: xMn^{2+}, yDy^{3+}, zEu^{3+} (x = 1, 2, 6, 8, 15 at%; y = 4 at%; z = 4 at%) phosphors excited with 365 nm LED.

green-yellow-red emission with the concentration ratio of Mn^{2+} to Dy^{3+} and Eu^{3++}, which contributes to the broad application field such as display, health and plant growth.

The photoluminescence mechanism of NaY(WO$_4$)$_2$: Mn^{2+}, Dy^{3+}, Eu^{3+}phosphor

From emission spectra it is obtained that the Mn^{2+}, Dy^{3+}, Eu^{3+} tri-doped in $NaY(WO_4)_2$ have meaningful influence on the tunable green-yellow-red LED. The energy levels of Mn^{2+}, Dy^{3+}, Eu^{3+} are shown in Fig. 5. With 365 nm exciting, the electrons are inspired to $^5D_4(Eu^{3+})$, and then transit from the $^5D_4$ (Eu^{3+}) to $^5G_4(Eu^{3+})$, $^5L_6$ (Eu^{3+}), $^5D_3(Eu^{3+})$, $^5D_3(Eu^{3+})$, $^5D_2(Eu^{3+})$, $^5D_1(Eu^{3+})$, $^5D_0(Eu^{3+})$ by the non-radiation transition. Finally, the electrons will move to the lower energy level of $^5D_0(Eu^{3+})$ to generate 613-617 nm red emission. The ^4D (Mn^{2+}) and $^4P(Mn^{2+})$ energy levels is near, which are all close to the energy level $^5D_4$ (Eu^{3+}). Also the energy level $^5D_4(Eu^{3+})$ is higher than the ^4D (Mn^{2+}) and $^4P(Mn^{2+})$, which make some of the electrons of Eu^{3+} transit from the $^5D_4(Eu^{3+})$ to ^4D (Mn^{2+}) and $^4P(Mn^{2+})$ by the cross relaxation. The electrons will continue transit from $^4D(Mn^{2+})$, $^4P(Mn^{2+})$ to $^4G(Mn^{2+})$, the green 546 nm can be obtained corresponding to the transition of $^4T_2(Mn^{2+}) \rightarrow {}^6A_1(Mn^{2+})$. Energy level of $^4G(Mn^{2+})$ is close to $^4F_{9/2}$ (Dy^{3+}), which will enhance the emission from $^4F_{9/2}$ (Dy^{3+}) to $^6H_{13/2}$ (Dy^{3+}), the 575 nm yellow emission. The energy level $^5D_4(Eu^{3+})$ is also higher than the $^4M_{19/2}$ (Dy^{3+}), which make some of the electrons of Eu^{3+} transit from the $^5D_4$ (Eu^{3+}) to $^4M_{19/2}$ (Dy^{3+}) by the cross relaxation. The electrons transit from the $^4M_{19/2}$ (Dy^{3+})^4 to $M_{21/2}$ (Dy^{3+}),$^4G_{11/2}$ (Dy^{3+}), $^4I_{15/2}$ (Dy^{3+}), $^4F_{9/2}$ (Dy^{3+}) by the non-radiation transition. Finally, the electrons will transit from $^4F_{9/2}$ (Dy^{3+}) to $^6H_{13/2}$ (Dy^{3+}) to generate the 575 nm yellow light.

Using the Tanabe-Sugano (T-S) theory [25], the energy levels of $3d^5$ ions is determined by the parameters of Dq, B and C. Dq is the strength of the octahedral crystal field, B and C are Racah parameters. The values of Dq, B and C are determined by the observed peaks of $^4T_1$ (^4G), $^4T_1$(^4P), and $^6A_1$ states, whose equations are shown as follows [26].

$$E(^6A_1 \rightarrow {}^4T_1(^4G)) = (-25B + 5C - 6\sqrt{5}\,Dq) - (-35B) \quad (2)$$

$$E(^6A_1 \rightarrow {}^4E_1(^4D) = (-18B + 5C) - (-35B) \quad (3)$$

From the absorption and emission spectra, we can obtain that the values of $E(^6A_1 \rightarrow {}^4T_1(^4G))$ = 18,315.0 cm^{-1} (546 nm), $E(^6A_1 \rightarrow {}^4E_1(^4D))$ = 27,397.3 cm^{-1} (365 nm), respectively. According to the T-S theory, generally, the C/B=4-6 and then here we select the C/B=5. And so, the parameters are calculated to be:

Dq = 337 ± 0.1 cm^{-1}, B = 652.3 ± 0.3 cm^{-1},
C = 3261.6 ± 0.7 cm^{-1}, Dq/B = 0.52 ± 0.01

In Fig. 5, the energy transition will be different with the Mn^{2+} doped in the micro-crystal structure. Also we can find the crystal field provides Dq/B=0.52 for the energy level split.

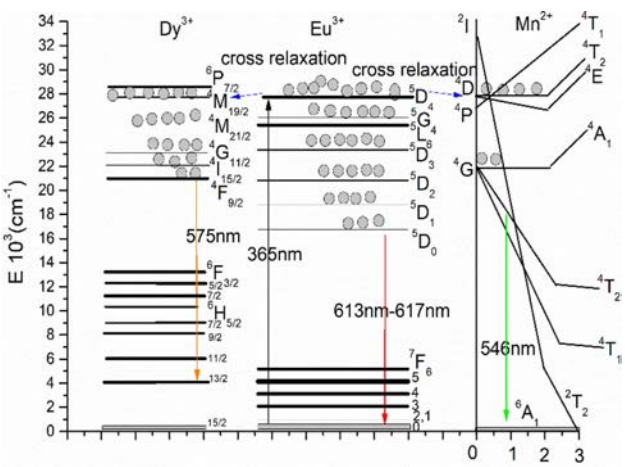

Fig. 5. Schematic illustration of Eu^{3+} to Mn^{2+} and Dy^{3+} energy levels in $NaY(WO_4)_2$: Mn^{2+}, Dy^{3+}, Eu^{3+}excited by 365 nm LED.

Conclusions

In summary, the $NaY(WO_4)_2$: xMn^{2+}, yDy^{3+}, zEu^{3+} (x = 1, 2, 6, 8, 15 at%; y = 4 at%; z = 4 at%) phosphors were successfully synthesized. The XRD pattern measured indicates it is well identical with the standard JCPDS #48-0886. The result of line-scanning SEM-EDS measured shows that the doped ions of Mn^{2+}, Dy^{3+} and Eu^{3+} are evenly distributed in the micro-crystal. The absorption and excitation spectra indicate that the 365 nm is suitable for the excitation source. The emission spectra excited with 365 nm LED are measured with different concentrations ratio of Mn^{2+} to Dy^{3+} and Eu^{3+}, it indicate that the 575 nm yellow emission and 546 nm green can be tunable with different concentrations of Mn^{2+}. And then, the 546 nm, 575 nm and 613-617 nm can be mixed to green-yellow-red light. The fluorescence mechanism is also presented, which imply that cross relaxation exist in the xMn^{2+}, yDy^{3+}, zEu^{3+}: $NaY(WO_4)_2$ (x = 1, 2, 6, 8, 15 at%; y = 4 at%; z = 4 at%) phosphors. And the high doped concentration of Mn^{2+} can guarantee the emission intensity of 546 nm enough. The result shows that the $NaY(WO_4)_2$: Mn^{2+}, Dy^{3+}, Eu^{3+} phosphors have good tunable green-yellow-red light with better performance. In this paper, commercial LED 365 nm light source is used for excitation, which makes the products easy to be commercialized, while most other products are fired by Xe-lamp, which is not conducive to commercial applications.

Acknowledgements

This study was funded by Natural Science Foundation

of Fujian Province (Grant Number 2018J01587).

Conflict of Interest

The authors declare that they have no conflict of interest.

References

1. C.G. Ming, F. Song, L.Q. An, and X.B. Ren, Curr. Appl. Phys.14[8] (2014) 1028-1030.
2. A.J. Peter and I.B. Shameem Banu, J. Mater. Sci. Mater. Electron. 28 (2018) 1-6.
3. M.T. Li, T. Takei, Q. Zhu, B.N. Kim, and J.G. Li, Inorg. Chem. 58[14] (2019) 9432-9442.
4. G. Li, J. Mater. Sci. Mater. Electron. 27[10] (2016) 11012-11016.
5. S. Sharma, N. Brahme, D.P. Bisen, and P. Dewangan, Opt. Express. 26[22] (2018) 29495-29508.
6. D.P. Dutta and P. Raval, J. Photochem. Photobiol. A 357 (2018) 193-200.
7. K.K. Rasu, D. Balaji, and S.M. Babu, J. Lumin. 170 (2016) 547-555.
8. B. Liu, J.J. Shia, Q.G. Wang, H.L. Tang, J.F. Liu, H.Y. Zhao, D.Z. Li, J. Liu, X.D. Xu, Z.S. Wang, and J. Xua, Opt. Mater. 72 (2017) 208-213.
9. Y.H. Jin, Y.H. Hu, L. Chen, G.F. Ju, H.Y. Wu, Z.F. Mu, M. He, and F.H. Xue, Opt. Mater. Express. 6[3] (2016) 929-937.
10. K. Li, H. Wang, X. Liu, W.M. Wang, and Z.Y. Fu, J. Eur. Ceram. Soc. 37[13] (2016) 4229-4233.
11. B.Y. Zhang, S.T. Ying, S.P. Wang, L.H, J.S. Zhang, and B.J. Chen, Inorg. Chem. 58[7] (2019) 4500-4507.
12. H. Ren, and F. Yang, J. Mater. Sci., Mater. Electron. 29[18] (2018) 15396-15403.
13. Q.M. Wei, J.P. Lu, G.C. Liu, and D.W. Liang, Spectrosc. Spect. Anal. 32 (2012) 3329-3334.
14. B. Han, B. Liu, Y. Dai, J. Zhang, and H. Shi, Ceram. Int. 45[3] (2019) 3419-3424.
15. S. Xu, Y. Xiang, Y.Q. Zhang, J.S. Zhang, X.P. Li, J.S. Sun, L.H. Cheng, and B.J. Chen, Sens. Actuators B Chem. 240 (2017) 386-391.
16. S.Y. Xiang, H. Zheng, Y.Q. Zhang, T.X. Peng, X.Q. Zhang, and B.J. Chen, J. Nanosci. Nanotechnol. 16[1] (2016) 636-642.
17. M.H. Li, L.L. Wang, W.G. Ran, Z.H. Deng, C.Y. Ren, and J.S. Shi, Ceram. Int. 43[9] (2017) 6751-6757.
18. Y. Yang, H. Feng, and X.G. Zhang, J. Mater. Sci. Mater. Electron. 26[1] (2015) 229-233.
19. Z.X. Shi, J. Wang, H. Jiang, X. Guan, Y. Lu, and J. Shi, J. Mater. Sci. Mater. Electron. 30[4] (2019) 3169-3176.
20. H.l. Song, Q. Han, C. Wang, X.Y. Tang, W.C. Yan, Y.F. Chen, X.R. Zhao, J.F. Jiang, and T.G. Liu, Opt. Mater. 78 (2018) 402-406.
21. A. Durairajan, D. Balaji, K.K. Rasu, S.M. Babu, M.A. Valente, D. Thangaraju, and Y. Hayakawa, J. Lumin. 170 (2016) 743-748.
22. Y.H. Wu, F.G. Yang, and F.P. Yan, J. Am. Ceram. Soc. 102[12] (2019) 7347-7354.
23. P.S. Mbule, B.M. Mothudi, and M.S. Dhlamini, J. Lumin. 192 (2017) 853-859.
24. T. Liu, Q.Y. Meng, and W.J. Sun, J. Alloy. Compd. 647 (2015) 830-836.
25. K. Ohkubo and T. Shigeta, J. Illum. Eng. Inst. 83[2] (1999) 87-93.
26. Y. Tanabe and S. Sugano, J. Phys. Soc. Jpn. 9[5] (1954) 766-799.